

AD-A087 523

CINCINNATI UNIV OHIO DEPT OF MATERIALS SCIENCE AND --ETC F/G 14/5  
ADAPTATION OF A KRATKY CAMERA TO USE WITH A ONE-DIMENSIONAL POS--ETC(U)  
AUG 80 R ROE, J C CHANG, M FISHKIS, J J CURRO N00014-77-C-0376

UNCLASSIFIED

TR-4

NL

1 of 1  
AD  
ADDITIONAL

END  
DATE  
FILMED  
9-80  
DTIC

ADA 087523

LEWIS

12  
B.S.

OFFICE OF NAVAL RESEARCH

Contract N00014-77-C-0376

Task No. NR 356-655

TECHNICAL REPORT NO. 4

Adaptation of a Kratky Camera to Use with a  
One-Dimensional Position Sensitive Detector

by

R. J. Roe, J. C. Chang, M. Fishkis and J. J. Curro

Prepared for Publication

in the

Journal of Applied Crystallography

Department of Materials Science and

Metallurgical Engineering

University of Cincinnati

Cincinnati, Ohio 45221

August 1, 1980

DTIC  
ELECTRONIC  
S AUG 6 1980  
A

Reproduction in whole or in part is permitted for  
any purpose of the United States Government

This document has been approved for public release  
and sale; its distribution is unlimited

80 8 4 105

DDC FILE COPY

REPORT DOCUMENTATION PAGE		READ INSTRUCTIONS BEFORE COMPLETING FORM
1. REPORT NUMBER Technical Report No. 4	2. GOVT ACCESSION NO. AD-A087523	3. RECIPIENT'S CATALOG NUMBER
4. TITLE (and Subtitle) Adaptation of a Kratky Camera to Use with a One-Dimensional Position Sensitive Detector.		5. TYPE OF REPORT & PERIOD COVERED Technical Report.
6. AUTHOR(s) Roe, J. C./Chang, M./Fishkis and J. J./Curro		7. PERFORMING ORG. REPORT NUMBER
8. PERFORMING ORGANIZATION NAME AND ADDRESS Dept. of Mat. Sci. & Met. Eng. ✓ University of Cincinnati Cincinnati, Ohio 45221		9. CONTRACT OR GRANT NUMBER(s) N00014-77-C-0376
10. CONTROLLING OFFICE NAME AND ADDRESS Office of Naval Research Arlington, VA 22217		11. REPORT DATE 1 August 1980
12. MONITORING AGENCY NAME & ADDRESS (if different from Controlling Office) 12 34 14 TR-4		13. NUMBER OF PAGES 22
14. DISTRIBUTION STATEMENT (of this Report) Approved for public release; distribution unlimited.		15. SECURITY CLASS. (of this report)
16. DISTRIBUTION STATEMENT (of the abstract entered in Block 20, if different from Report)		
17. SUPPLEMENTARY NOTES Prepared for publication in the Journal of Applied Crystallography.		
18. KEY WORDS (Continue on reverse side if necessary and identify by block number) Small-angle X-ray scattering, one-dimensional position sensitive detector, Kratky camera.		
19. ABSTRACT (Continue on reverse side if necessary and identify by block number) A Kratky small-angle x-ray camera was modified so as to allow the use of a one-dimensional position sensitive detec- tor with it. The modification was designed in such a way that most of the calibrations, necessary for subsequent cor- rection of the collected intensity data, can be performed with little alteration in the collimation geometry or the electronics settings. In particular, the calibration of the		



Adaption of a Kratky Camera to  
Use with a One-Dimensional Position  
Sensitive Detector

by

Ryong-Joon Roe, J. C. Chang,  
M. Fishkis and J. J. Curro  
Department of Materials Science and  
Metallurgical Engineering  
University of Cincinnati  
Cincinnati, Ohio 45221

### ABSTRACT

A Kratky small-angle x-ray camera was modified so as to allow the use of a one-dimensional position sensitive detector with it. The modification was designed in such a way that most of the calibrations, necessary for subsequent correction of the collected intensity data, can be performed with little alteration in the collimation geometry or the electronics settings. In particular, the calibration of the uniformity of detector efficiency can be performed by repeated vertical travel of the detector at a constant speed across a beam scattered from a sample. A much higher speed of data collection, with no increase in the background noise nor any loss in the angular resolution, has been achieved in comparison to a regular Kratky camera operating in step-scanning mode. The practical utility of combining the PSD with a Kratky camera for studies of isotropic samples has been demonstrated.

## I. INTRODUCTION

In the past decade position sensitive detectors (PSD) for x-ray measurements have been developed in several laboratories. Some of the one-dimensional detectors are now available commercially from several sources. The time required for collecting x-ray data with the use of these detectors is reduced typically by an order of magnitude in comparison to the time taken when a conventional proportional counter is used in step-scanning.

Earlier, Schelten and Hendricks (1978) investigated the combination of a one-dimensional PSD with a rotating anode x-ray generator and a pin-hole collimation, and showed that the accuracy of the data and the speed of data collection obtainable with such a combination compare very favorably to those attainable with a traditional arrangement of a Kratky camera fitted with a proportional counter, but with the additional advantage of not requiring a correction for slit-smearing. For investigation of isotropic samples, another way of utilizing the advantage of a one-dimensional PSD is to retain the Kratky collimation and instead replace the proportional counter, traditionally used in step-scanning mode, with a one-dimensional PSD. In a recent article Russell et al. (1979) discussed their effort to combine a LDPSD with a Kratky camera and gave a detailed account of their design considerations and the results of its performance test. In our laboratory, we also made modifications to a Kratky camera for the purpose of adapting it to use with a LDPSD, and it has been in use satisfactorily in the past few years. In this article we give a brief

description of the modifications, in order to share our experience with others who might plan similar adaptation of a Kratky camera.



## II. MODIFICATION OF KRATKY CAMERA

### A. Detector

We used a one-dimensional PSD purchased from Tennelec Inc., Oak Ridge, TN. This is a gas-flow proportional counter having a carbon-coated quartz wire as the anode. The position of the ionization event induced by the incoming photon, detected on the wire, is determined by the method of RC line encoding (Borkowski and Kopp, 1970, 1972, 1975), i.e., by comparison of the rise times of the two pulses emanating from each end of the anode wire. The dimension of the active detector window is 4 mm x 80 mm. The positional resolution capability is rated at 200  $\mu$ m for 8 KeV x-rays. Although our experience is confined to the use of this particular detector, most of the considerations given below should apply also to the use of a 1DPSD of other make or design.

### B. Sample-to-Detector Distance

The angular resolution of the instrument increases in proportion to the sample-to-detector distance  $L$ , while the intensity at the detector falls as  $1/L$  in the case of slit collimation. The optimum value of  $L$  is set by the compromise of these two conflicting requirements. We chose 50 cm for  $L$  in our design from the following considerations. The detector-pre-amplifier assembly is about 20 cm high and cannot be mounted on the track (T in Fig. 1) on which other components of the Kratky camera are mounted. When the detector is mounted immediately beyond the end of the track,  $L$  turns out to be about 50 cm. When an entrance slit of width  $W_1$  is used, the primary beam

spreads to a width  $W_p$  at the detector registration plane, with  $W_p$  given by

$$W_p = \frac{L + D}{6} W_1$$

where  $D$  is the distance from the entrance slit to the sample and both  $L$  and  $D$  are in cm. With the camera we use  $D$  is equal to 17.5 cm. Therefore with  $L = 50$  cm,  $W_p/W_1$  is equal to about 10. When a 60  $\mu\text{m}$  entrance slit is used,  $W_p$  is about 600  $\mu\text{m}$ , which is far larger than the positional resolution limit of the detector. Increasing  $L$  beyond 50 cm will simply increase the width of the primary beam at the detector and gain very little in angular resolution. In addition to decreasing the intensity at the detector, an increase in  $L$  brings about another undesirable effect. The distribution of intensity in the primary beam at the detector plane, in the horizontal direction perpendicular to the beam axis, is the slit length weighting function determining the effect of slit length smearing. In a well-aligned Kratky camera, the measured slit length weighting function is usually a trapezoid with the top edge sufficiently wide to allow infinite slit approximation. For a given collimation geometry and a finite length of the focal spot, increasing  $L$  causes the width of the trapezoid top edge to become smaller, eventually making the infinite slit approximation invalid. In short, in our design the value of  $L$  was chosen to be 50 cm because it was the shortest distance, which was mechanically convenient to achieve, without compromising other collimation requirements. In fact, for most of our studies an entrance slit of 100  $\mu\text{m}$  or wider is used, and in these cases the angular resolution of the data is

limited by the collimation geometry itself and not by the resolution capability of the detector.

C. Modification Design

From the original Kratky camera the tapered rear vacuum chamber, with the adjustable receiving slit and the detector mounting device, was removed and in its place was fitted a new vacuum chamber with a detector mount attached at its rear. The vacuum chamber was fabricated from a steel tubing of a rectangular cross-section 3 inches by 6 inches and cut to a length of ca. 30 cm. A steel plate, with appropriate openings and screw holes machined in, was welded to each end of the tubing, and then the whole vacuum chamber was heavily nickel-plated to prevent Fe fluorescence. At the center of the rear end plate a vertical slot of 9 mm width and 7 cm height was cut out as the beam exit. A beam stop (made of Ta sheet rather than W because of the ease of machining the former) was attached at the lower end of the slot from the inside of the vacuum chamber. The slot was then sealed with a thin Mylar film to hold vacuum.

As shown in Fig. 1, the front part of the vacuum chamber is supported by the pivot U, while its rear is supported by its being resting on top of the movable steel column at the center of the "angular device" W. This angular device is the one provided in the original Kratky camera for effecting vertical motion of the receiving slit, and the worm gear attached to the knurled knob actuates the central cylindrical column to move precisely up and down. The beam stop attached to the rear end plate of the vacuum chamber is brought to the correct position by raising or lowering

the rear end of the vacuum chamber as a whole by means of the angular device W.

The detector mount itself consists of two parts. The connector plate X is attached with screws to the rear end plate of the vacuum chamber, and has a vertical slot in its center (not visible in Fig. 1) for inserting a beam attenuator or an auxiliary slit for calibration purposes. A precision linear slide Y is clamped in the connector plate in such a way that its vertical position can be readily altered. The precision slide Y consists of a vertical frame with a mm scale marking and a slide plate movable within the frame, the slide plate capable of being translated up and down by means of a long central screw. The range of travel is 20 cm. The detector itself is attached to the movable slide plate. By means of a synchronous motor connected to the screw, the detector can be moved up and down at a constant speed (3 cm/min.). With the help of limit switches placed at the top and bottom ends of the travel, the up and down motion of the detector can be repeated unattended. This motorized device is for the purpose of calibrating the detector efficiency curve as explained below. By means of a manual switch the detector position can also be altered readily, and its position read off the mm scale marking.

### III. DETECTOR CALIBRATION

Calibration of the detector is necessary with respect to three aspects: spacial linearity, energy resolution and detection efficiency. Although the spacial resolution of the detector is of interest when the performance of the detector is to be compared and tested, it is not required for the purpose of correcting the collected scattered intensity data. For the latter purpose what is required is the determination of the primary beam profile at the detector registration plane which reveals the combined effect of the collimation error and the detector resolution error. Determination of the primary beam width profile is discussed briefly in Section IV.

#### A. Spacial Linearity

A strongly scattering sample was placed in the sample holder, and an auxiliary slit was placed in the slot in front of the detector so that the angular range of the scattered intensity entering the detector was very narrowly limited. The channel number of the peak position in the multichannel analyzer (MCA) displaying the intensity profile was noted, together with the position of the detector as read from the mm scale marking on the slide. Such measurements were repeated after altering the position of the detector by means of a manual switch actuating the slide motor. The plot of the channel number of the peak in the MCA against the position of the detector deviated very little from a straight line. It was concluded that a correction for spacial linearity would not be necessary for subsequent measurements. From the slope of the linear plot it was determined that 1 cm

on the detector corresponded to 36.5 channels on the MCA under the conditions employed.

#### B. Energy Resolution

The detector energy resolution can be determined readily by taking the sum of the pulses coming from the two ends of the detector and feeding it into the MCA input, and thereby directly displaying the energy spectrum. We determined the energy resolution for a short section of the anode wire at a time. With Ni-filtered  $\text{CuK}\alpha$  radiation falling on a strongly scattering sample, the scattered beam was received on a 5 mm section of the detector defined by means of an auxiliary slit inserted in its front. The value of the energy resolution (the ratio of the FWHM to the peak position) thus determined in the mid-section of the detector was 25-26%, a value slightly larger than expected of a conventional proportional counter. Toward the ends of the detector the resolution deteriorated to around 29%. More important to note, however, was the fact that the channel number in the MCA (i.e., the voltage) of the peak in the energy spectrum varied significantly when different sections of the detector wire were examined. Through the length of the detector, the total variation was as much as 9%. The overall energy resolution is therefore much poorer than 26%, and the voltage window in the single channel analyzer in the energy discrimination circuit had to be opened wider than would normally be employed with a proportional counter.

#### C. Detection Efficiency

Ideally the efficiency of detecting incoming photons should be uniform along the total length of the detector. In practice

the detection efficiency is not uniform for a variety of reasons, for example, due to non-uniformity of the resistance of the anode wire, slight variations in the position of the wire in the detector chamber, etc. The observed raw data, the number of counts vs. channel number, have to be divided by the relative efficiency of each channel to obtain a true variation of the scattered intensity with angle. The detection efficiency correction is probably the most crucial step in the use of a PSD to obtain reliable data of high precision. Calibration of the detection efficiency curve has to be performed fairly often because of the following reasons. 1) The efficiency curve is very sensitive to the various settings in the detector electronic circuitry such as the bias voltage, the amplifier gain, the energy discriminator window, etc. As the electronic components age their values drift slowly and may then alter the efficiency curve. 2) The carbon coating on the quartz anode wire erodes with usage. Accidental exposure of a section of the wire to a primary x-ray beam can damage that part immediately. A prolonged exposure to strong scattered beam can, however, also eventually lead to permanent erosion of that section of the wire. Faruqi (1975) observed that detection of ca.  $2 \times 10^7$  photons over a  $100 \mu\text{m}$  section of the wire resulted in a significant loss of spacial resolution. Our experience has been that the section of the wire exposed consistently to a higher intensity part of the scattered beam eventually developed a dip in the efficiency curve. Once a dip becomes noticeable, a further deterioration is fairly rapid, leading to an almost total loss of detection capability at that

section and also to a distortion of the efficiency curve in the neighboring sections as well. It is probable that the factor determining the erosion is not the accumulated number of photons detected, but rather the accumulated number of ions collected. Whenever the nature of the sample and the problem of study was such that a high spatial resolution was not essential, we therefore operated the detector at a lower gas gain, compensating it with a higher electronic amplification. The lower gas gain gives rise to a smaller number of ions collected for each photon detected, while as a trade-off suffering some loss in the spatial resolution because of the enhanced noise arising from the higher electronic amplification. When a section eventually eroded, we simply shifted the detector position to avoid the use of that section; the useful life of the detector was prolonged in this way since the usable length of the detector was originally much longer than required for our purpose (5 cm for measurements up to  $2\theta = 0.1$  radian).

The detection efficiency calibration was performed as follows. A strongly scattering sample was placed in the sample holder in the camera. An auxiliary slit was inserted in front of the detector to allow only the high intensity (low angle) part of the scattered intensity to illuminate a 1 cm section of the detector. The detector was then let to travel up and down at a constant speed, so that every section of the detector wire was exposed equally to the x-ray beam. The limit switches were set in such a way that the reversal of travel direction occurred only when the usable section of the wire had passed way beyond the



opening in the auxiliary slit. This up-and-down travel of the detector, operating automatically, was continued several hours, with the x-ray generator at its full power, until a sufficient number of counts at each MCA channel were accumulated to make the statistical scatter tolerably small.

Fig. 2 shows two observed efficiency curves obtained in this manner. They were rescaled to an average of unity for the purpose of comparison. The two curves were obtained at about a month's interval, under identical conditions except that the detector bias voltage was altered from -2330 to -2350 volts. The rather pronounced difference between the two curves arises from the following effect. As the bias voltage was made more negative, the gas amplification factor increased, and as a result the voltage of the pulses fed into the single channel analyzer in the energy discriminator channel was all enhanced by the same factor. Since the energy discriminator window was left fixed, the fraction of pulses admitted through the gate was now altered. The change in the detection efficiency, caused by this relative change of the energy discriminator window against the average pulse voltage, affects different sections of the detector differently. Those sections of the detector, which previously generated undersized pulses on the average, now experiences an apparent increase in the detection efficiency, while other sections of the detector shows deterioration of the efficiency because the mismatch of the energy window becomes now more pronounced.

#### IV. BEAM WIDTH PROFILE AND ZERO OF ANGLE

The primary beam width profile (i.e., the intensity distribution in the vertical direction) is required to determine the zero of the scattering angle  $2\theta$  (defined as the center of the mass of the intensity distribution) and also for the purpose of correcting the observed intensity data for the width smearing effect. For this purpose the beam stop affixed to the rear-end of the vacuum chamber is lowered below the primary beam by turning the knob on the angular device W (see Fig. 1). With the primary beam attenuated with an appropriate thickness of Ni foil, the beam width profile is then measured directly with the PSD. As the beam stop is subsequently raised into position by raising the rear end of the vacuum chamber as a whole, the detector also is lifted and the MCA channel number corresponding to the zero angle changes. The relation between the motion of the central screw in the angular device W (indicated on the scale engraved thereon) and the shift in the channel number was previously established, and therefore the channel number for the beam zero can be calculated from the reading of the scale on the angular device W. Fig. 3 shows the beam width profile obtained with a 44  $\mu\text{m}$  entrance slit and another with a 120  $\mu\text{m}$  entrance slit. Also shown in Fig. 3, for comparison, is the beam width profile obtained with a conventional proportional counter in step-scanning mode on a standard Kratky camera, in which the entrance and receiving slit widths were 60 and 150  $\mu\text{m}$  respectively and the sample-to-detector distance was 210 mm. It shows that the beam width obtained with a 100  $\mu\text{m}$  entrance slit and a 1DPSD would be

comparable to that obtainable with a 60  $\mu\text{m}$  entrance slit in a conventional Kratky camera.

For the sake of completeness, we show in Fig. 4 the observed primary beam length profile (the horizontal intensity distribution). For this measurement the vacuum chamber had to be removed, and the detector was mounted at about the same position (right behind the camera track) by means of a separately constructed device. This device had a detector mount which moves on a slide plate to let the detector displaced in the horizontal direction (perpendicular to the beam axis) and the detector position could be read off a scale marking on the slide frame. In principle the beam length profile is determined mostly by the front collimation geometry and very little change is to be effected when a conventional proportional counter is replaced by a LDPSD. It nevertheless is preferable to determine the length profile with the same detector and with the camera geometry as nearly the same as possible as are employed in the subsequent measurement of the intensity scattered by the samples. The beam length profile can also be calculated from the collimation geometry and good agreements of the calculated with the measured profiles are often claimed, but the measured profile, if available, is still preferable to a calculated one.

## V. DISCUSSION

As a simple illustration of the performance of the camera, we present in Fig. 5 the intensity data obtained with a Lupolen polyethylene sample. This is a sample calibrated and kindly supplied by Prof. O. Kratky as a secondary standard for measurement of primary beam intensity (see Kratky, Pilz and Schmitz, 1966). The equipment and operating conditions employed for the data in Fig. 5 are: Philips generator XRG 3100 at 45 KV 40 mA, a Philips broad focus Cu tube (nominal focal spot size 2 mm x 12 mm), a Ni-filter and a 120  $\mu$ m entrance slit. Argon gas with 10% methane was used in the PSD at a pressure of 75 psi. Also shown in Fig. 5 is the result of the blank run made without a sample. The "background" intensity level thus obtained is very low, indicating the absence of fluorescence or any adverse reflection of the primary beam. The Kratky camera used for this measurement is the one modified by Hendricks (1970) to eliminate the Mylar windows in the front and rear of the sample holder by interconnecting the vacuum chambers with metal bellows. Because of this, the background count level realized here might be slightly lower than can be obtained with an ordinary Kratky camera.

The data shown in Fig. 5, both the scattering from the Lupolen sample and the blank run, were collected for 10 min. At the scattering angle 10.2 milliradian (corresponding to 150 Å), a count rate of 70 counts per second results in the accumulated counts of 40,000 in 10 min., giving a statistical error of 0.5%. For some types of studies, for example, kinetics of phase

transitions, a statistical error of this magnitude could be entirely tolerable. The measurement time could be reduced further by an order of magnitude by introduction of several modifications. By using Xe instead of Ar as the fill gas of the PSD, the detection efficiency can be increased by a factor of 2. If the nature of the structural features in the sample is such that a further loss in spatial resolution can be tolerated, the entrance slit width may be increased to 150 - 200  $\mu\text{m}$ , with attending gain in the count rate by a factor of 2 to 3 (which depends on the size of the focal spot on the x-ray tube). By use of a rotating anode rather than a sealed x-ray tube, the intensity can be increased by a factor of 3 - 10 (which of course depends on the power rating of the generator).

When such modifications are introduced, it should become feasible to collect a fairly decent intensity data, even better than shown in Fig. 5, in a period of about a minute. We have made some study of the kinetics of thermally induced phase change of block copolymers with our present system, and find that our capability of following the process is limited rather by the speed at which we can alter the temperature of the sample from one to another isothermal condition, and also by the speed at which the data in the MCA are transferred to a computer.

The higher count rates, which might be achieved by the modifications suggested above, are likely to strain the capacity of the PSD in two respects. First, the erosion of the carbon-coated quartz wire will be so much faster, necessitating more frequent calibration of the detection efficiency curve and

earlier replacement of the anode wire. Secondly, the count-rate capability of the LDPSD's commercially available at present (including the one we use) is rated at  $2 - 10 \times 10^4$  counts per second. This count-rate limitation arises mainly because the space-charge of ions builds up faster than can be drained off by neutralization at the electrodes. The effect would therefore be more severe at the particular section of the detector receiving higher intensity than the rest. The design principles to overcome these limitations are known, and a LDPSD incorporating these principles may become available even commercially in due time.

## VI. CONCLUSION

For studies of isotropic samples, coupling a one-dimensional PSD with a Kratky collimating system is an eminently useful approach. The inherent advantage of a PSD, i.e., the speed of data collection, is fully realized by this combination. The spatial resolution of 200  $\mu\text{m}$ , realizable in currently available PSD's, is probably adequate for most studies except when structural features much larger than 1000  $\text{\AA}$  are investigated.

An important advantage of using a PSD is that it does not require a highly stabilized x-ray power supply, thus making the use of a rotating anode tube practicable. Balancing against this advantage is the fact that the collected intensity data have to be corrected for the non-uniform detection efficiency along the length of the detector. Because the detection efficiency curve could drift with time, our instrument was designed with a view to making the calibration of the detection efficiency convenient and accurate. We avoided the use of a  $\text{Fe}^{55}$  isotope as a radiation source for calibration purpose, because  $\text{MnK}\alpha$  radiation emanating from  $\text{Fe}^{55}$  necessitates alteration in the settings of the electronics, and it would seem difficult to assure that the response of the detector under this altered condition would be exactly the same as its response toward  $\text{CuK}\alpha$  in the normal use. In fact in our design attention was paid to enable various calibrations to be performed with very little alteration in the electronics and collimation geometry from what will be used in subsequent measurements with samples of interest.

ACKNOWLEDGMENT

This work has been supported in part by the Office of Naval Research. We gratefully acknowledge the loan of the Kratky camera used in this work by the Oak Ridge National Laboratory.



#### REFERENCES

- Borkowski, C. J. & Kopp, M. K. (1970) IEEE Trans. Nucl. Sci. NS17, 340-349.
- Borkowski, C. J. & Kopp, M. K. (1972) IEEE Trans. Nucl. Sci. NS19, 161-168.
- Borkowski, C. J. & Kopp, M. K. (1975) Rev. Sci. Instr. 46, 951-962.
- Faruqi, A. R. Proc. 2nd ISPRA Nucl. Electronics Symposium, May, 1975, 199-204.
- Hendricks, R. W. (1970) J. Appl. Cryst. 3, 348-353.
- Kratky, O., Pilz, I. & Schmitz, P. J. (1966) J. Colloid Interface Sci. 21, 24-33.
- Russell, T. P., Stein, R. S., Kopp, M. K., Zedler, R. E., Hendricks, R. W. & Lin, J. S. (1979) Oak Ridge National Laboratory Technical Memorandum 6678.
- Schelten, J. & Hendricks, R. W. (1975) J. Appl. Cryst. 8, 421-429.

## LEGEND TO FIGURES

Fig. 1 Photograph of the modified part of the Kratky camera. The vacuum chamber V, made from a steel tubing of 3 inch by 6 inch rectangular cross section and heavily Ni-plated, is supported by the pivot U and the "angular device" W. The detector connector plate X has a slot to accommodate an auxiliary slit for calibration purposes, and supports the linear slide Y. The detector is mounted on the movable slide plate, which can be made to travel up and down by means of the motor M.

Fig. 2 Comparison of two calibration curves of the detector efficiency against the MCA channel number. The curves were obtained at the detector bias voltage of -2330 and -2350 volts. The rather pronounced change in the detector efficiency curve arises from the energy discriminator window affecting different channels slightly differently.

Fig. 3 The primary beam width profiles, measured with the one-dimensional PSD, are shown in (a), the entrance slit used being of width 44  $\mu\text{m}$  and 120  $\mu\text{m}$  for the two curves shown. Shown in (b) for comparison is the primary beam width profile obtained with an ordinary proportional counter in a regular Kratky camera having a 60  $\mu\text{m}$  entrance slit and 150  $\mu\text{m}$  receiving slit.

Fig. 4 The primary beam length profile, measured with the PSD mounted in the normal position but with the vacuum chamber removed.

Fig. 5 The intensity ( $\Delta$ ) scattered from a Lupolen sample (a calibrated polyethylene sample kindly provided by Prof. O. Kratky) and the "background" scattering (X) obtained under the same instrumental conditions. The counts were accumulated for 10 min. in each case.

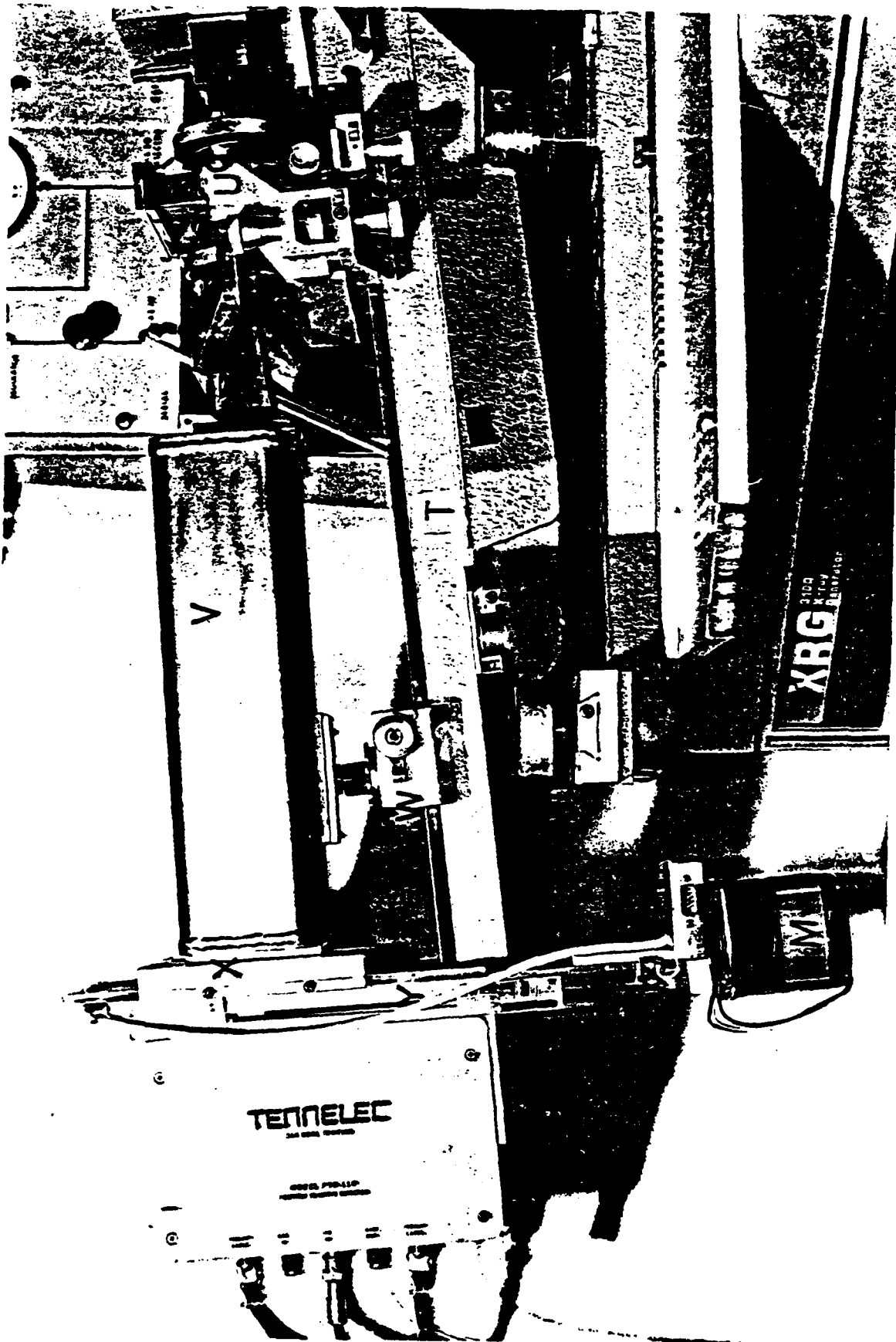
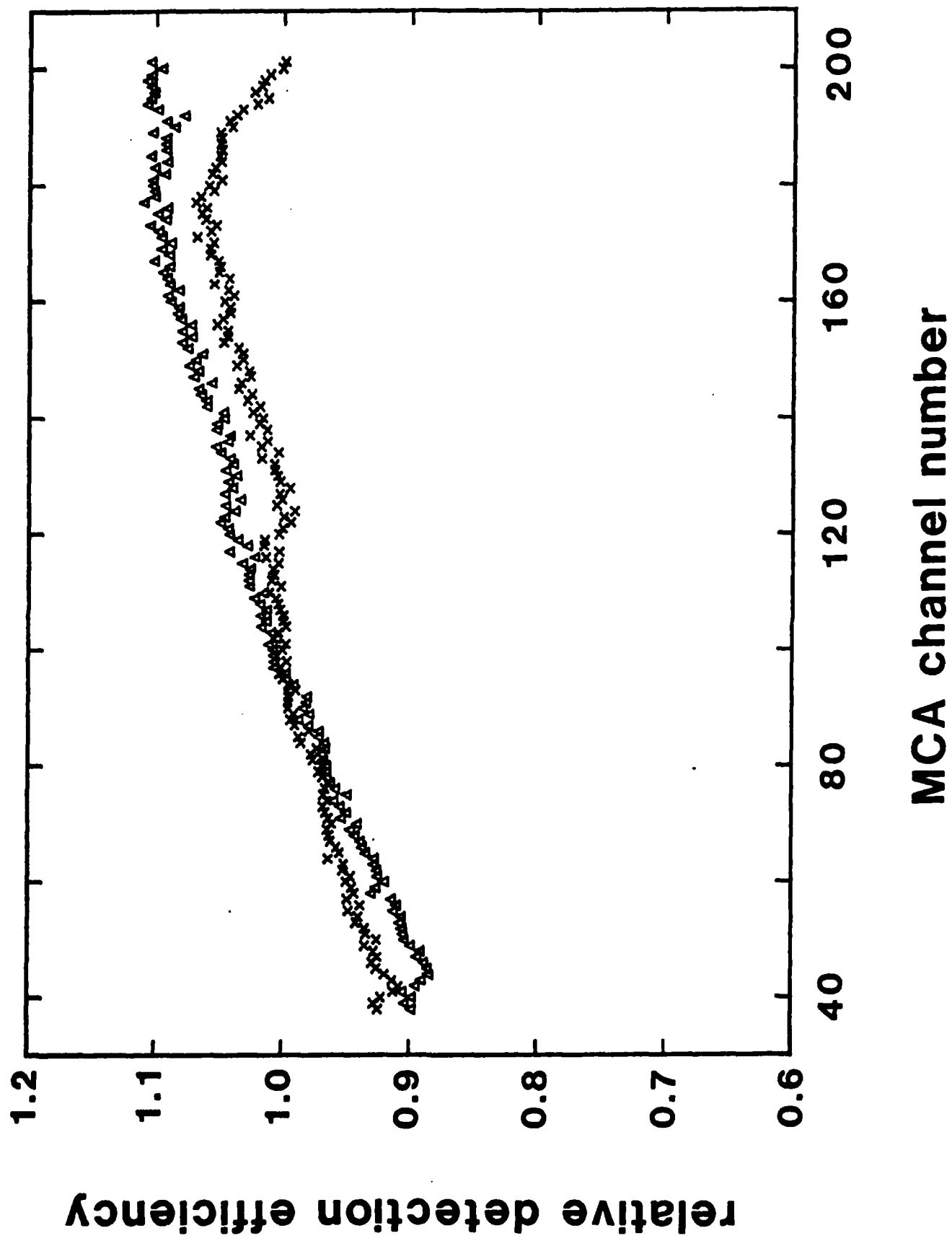


FIG 1

FIG 2



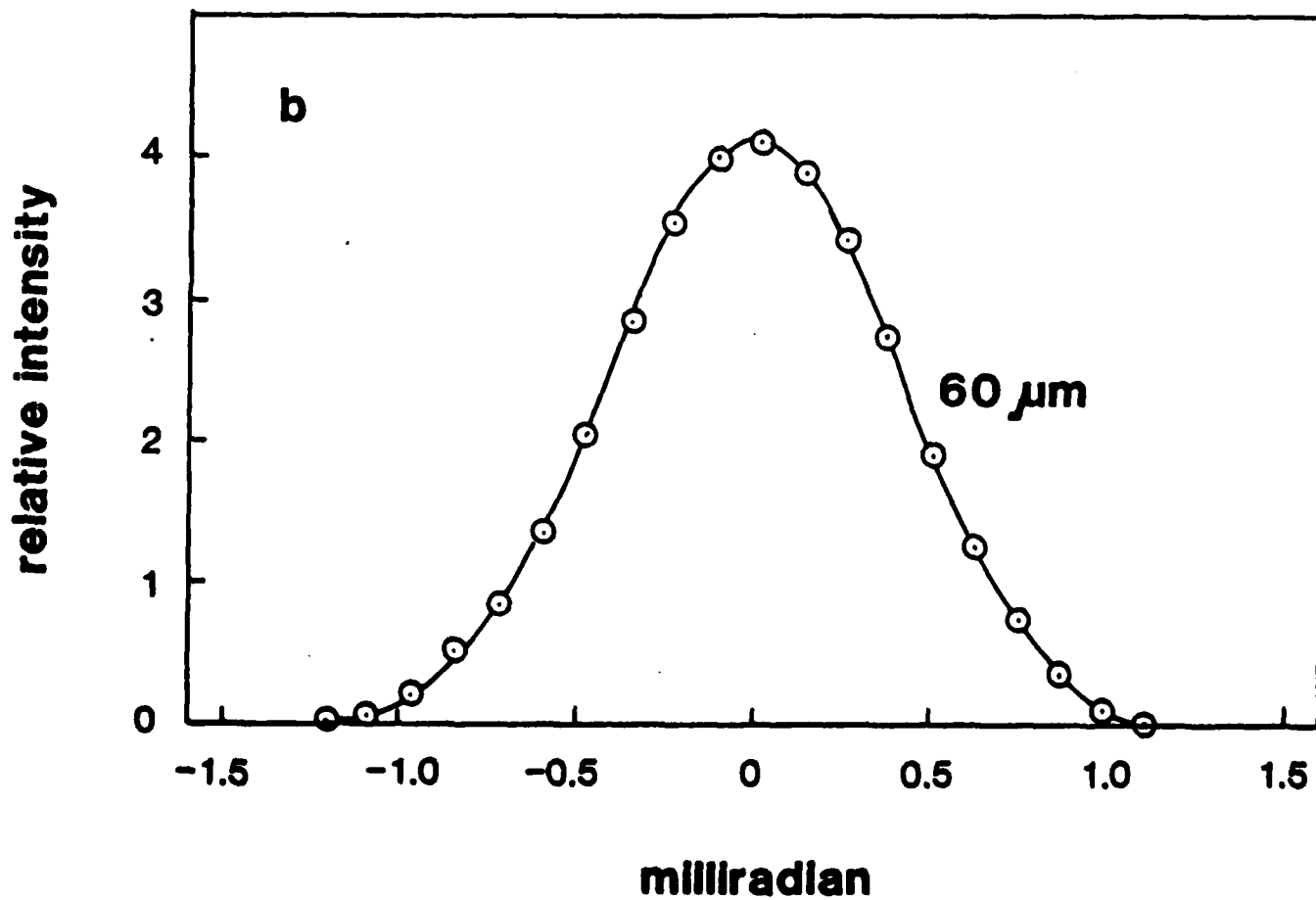
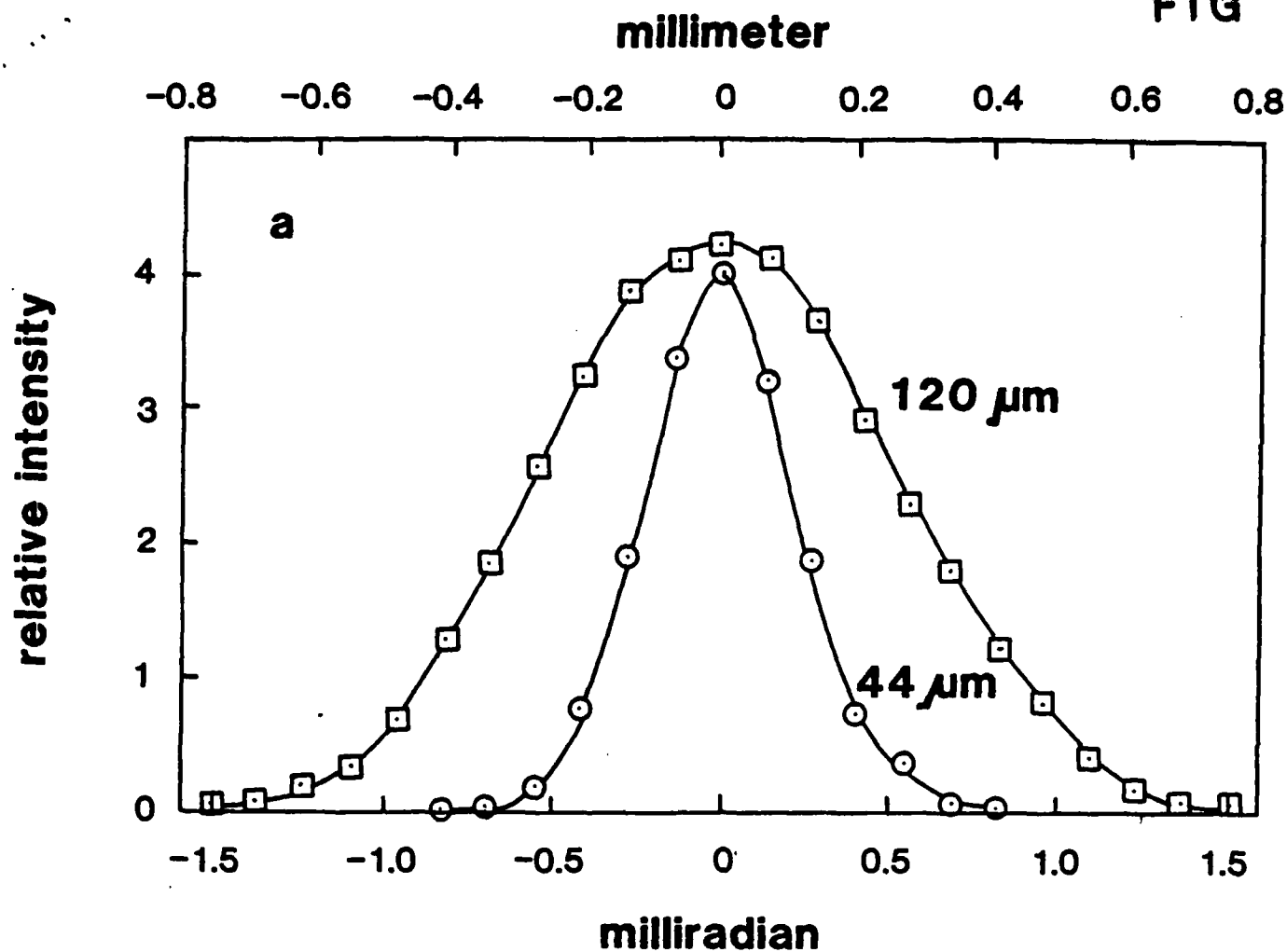


FIG 4

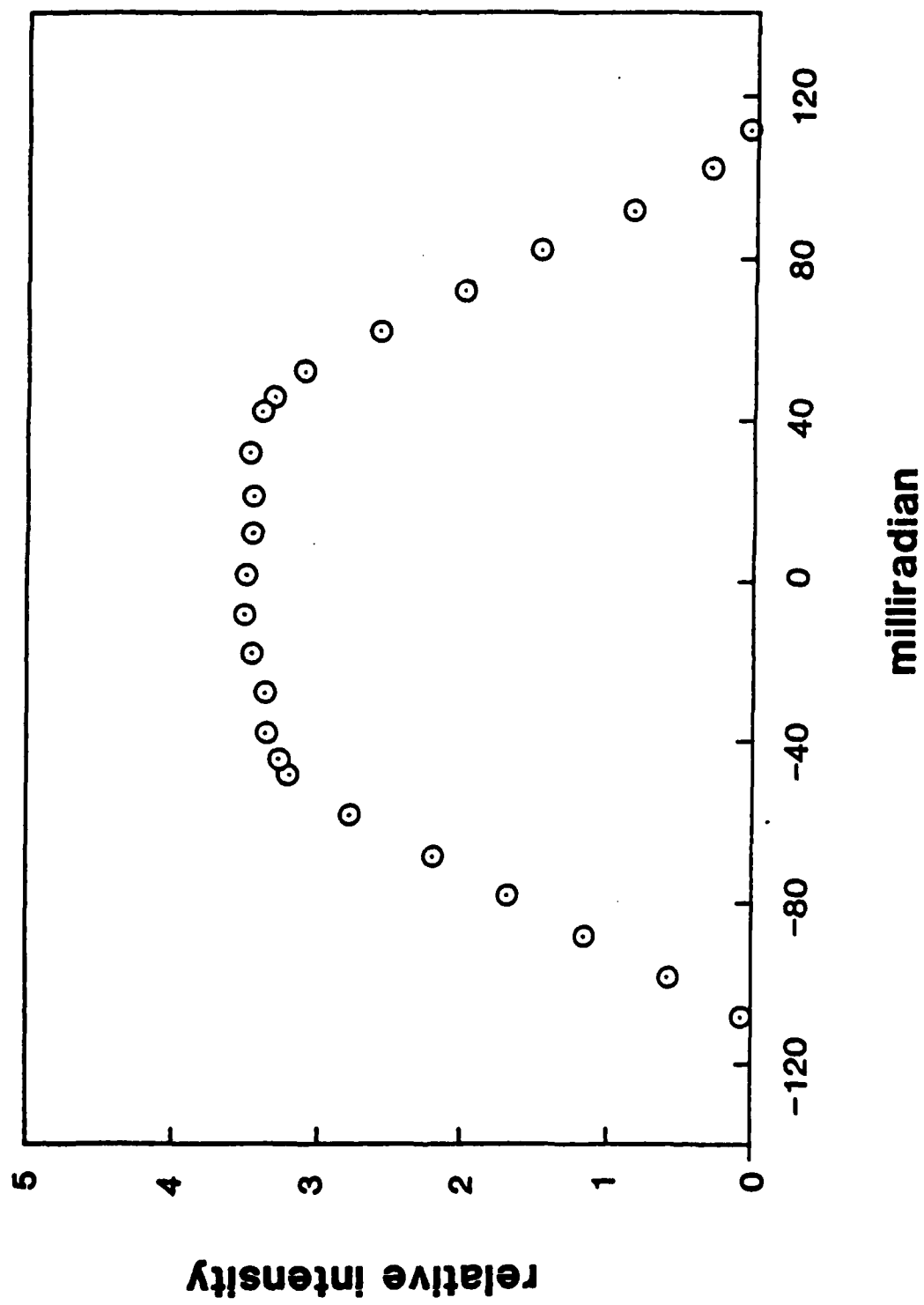
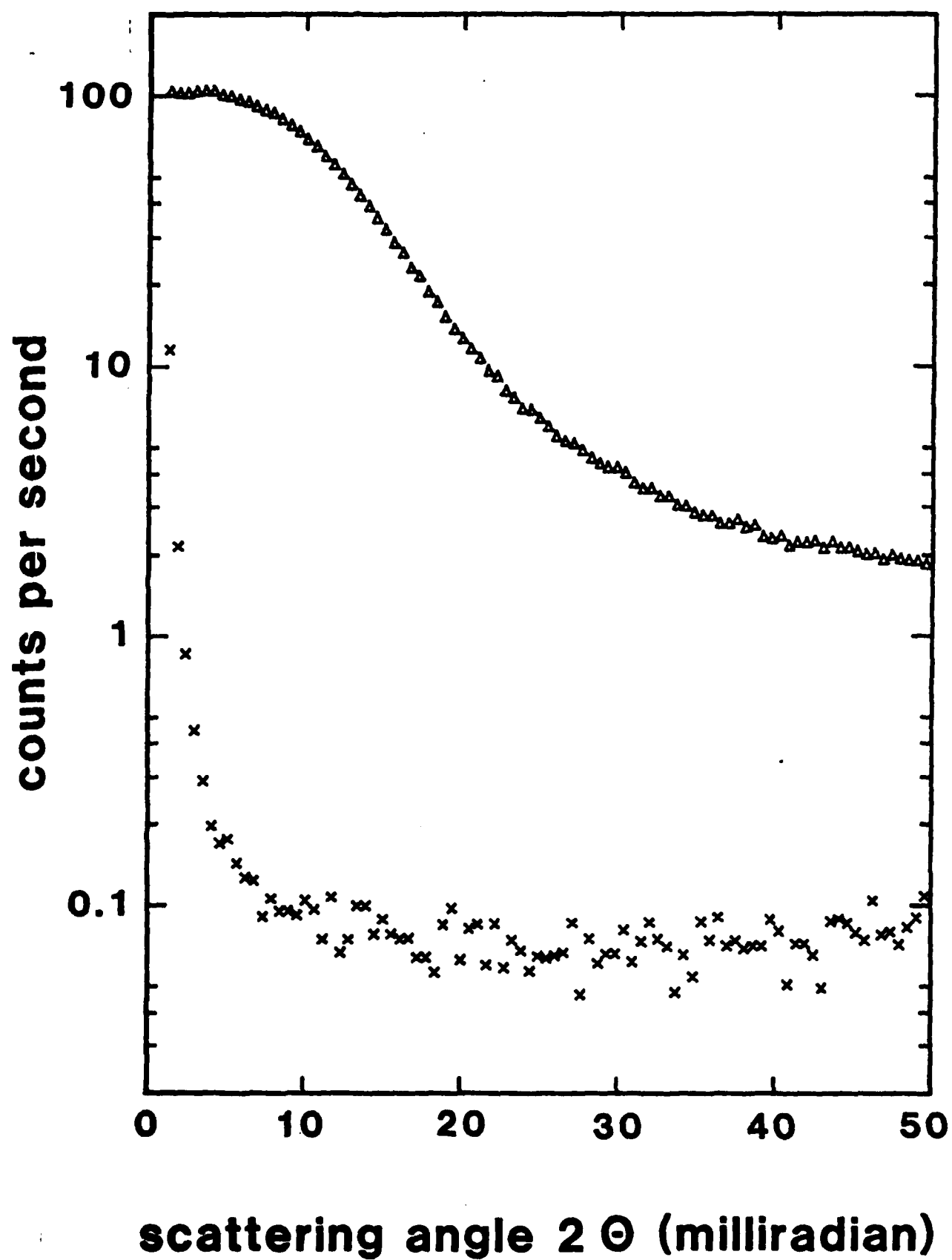


FIG 5



TECHNICAL REPORT DISTRIBUTION LIST, GEN

	<u>No.</u> <u>Copies</u>		<u>No.</u> <u>Copies</u>
Office of Naval Research Attn: Code 472 800 North Quincy Street Arlington, Virginia 22217	2	U.S. Army Research Office Attn: CRD-AA-IP P.O. Box 1211 Research Triangle Park, N.C. 27709	1
ONR Branch Office Attn: Dr. George Sandoz 536 S. Clark Street Chicago, Illinois 60605	1	Naval Ocean Systems Center Attn: Mr. Joe McCartney San Diego, California 92132	1
ONR Branch Office Attn: Scientific Dept. 715 Broadway New York, New York 10003	1	Naval Weapons Center Attn: Dr. A. B. Amster, Chemistry Division China Lake, California 93555	1
ONR Branch Office 1030 East Green Street Pasadena, California 91106	1	Naval Civil Engineering Laboratory Attn: Dr. R. W. Drisko Port Hueneme, California 93401	.
ONR Branch Office Attn: Dr. L. H. Peebles Building 114, Section D 666 Summer Street Boston, Massachusetts 02210	1	Department of Physics & Chemistry Naval Postgraduate School Monterey, California 93940	1
Director, Naval Research Laboratory Attn: Code 6100 Washington, D.C. 20390	1	Dr. A. L. Slafkosky Scientific Advisor Commandant of the Marine Corps (Code RD-1) Washington, D.C. 20380	1
The Assistant Secretary of the Navy (R,E&S) Department of the Navy Room 4E736, Pentagon Washington, D.C. 20350	1	Office of Naval Research Attn: Dr. Richard S. Miller 800 N. Quincy Street Arlington, Virginia 22217	1
Commander, Naval Air Systems Command Attn: Code 310C (H. Rosenwasser) Department of the Navy Washington, D.C. 20360	1	Naval Ship Research and Development Center Attn: Dr. G. Bosmajian, Applied Chemistry Division Annapolis, Maryland 21401	1
Defense Documentation Center Building 5, Cameron Station Alexandria, Virginia 22314	12	Naval Ocean Systems Center Attn: Dr. S. Yamamoto, Marine Sciences Division San Diego, California 91232	1
Dr. Fred Saalfeld Chemistry Division Naval Research Laboratory Washington, D.C. 20375	1	Mr. John Boyle Materials Branch Naval Ship Engineering Center Philadelphia, Pennsylvania 19112	1



TECHNICAL REPORT DISTRIBUTION LIST. GENNo.  
Copies

Dr. Rudolph J. Marcus  
Office of Naval Research  
Scientific Liaison Group  
American Embassy  
APO San Francisco 96503

1

Mr. James Kelley  
DTNSRDC Code 2803  
Annapolis, Maryland 21402

1

TECHNICAL REPORT DISTRIBUTION LIST, 356A

	<u>No.</u> <u>Copies</u>		<u>No.</u> <u>Copies</u>
Dr. Stephen H. Carr Department of Materials Science Northwestern University Evanston, Illinois 60201	1	Picatinny Arsenal SMUPA-FR-M-D Dover, New Jersey 07801 Attn: A. M. Anzalone Building 3401	1
Dr. M. Broadhurst Bulk Properties Section National Bureau of Standards U.S. Department of Commerce Washington, D.C. 20234	2	Dr. J. K. Gillham Princeton University Department of Chemistry Princeton, New Jersey 08540	1
Dr. T. A. Litovitz Department of Physics Catholic University of America Washington, D.C. 20017	1	Douglas Aircraft Co. 3855 Lakewood Boulevard Long Beach, California 90846 Attn: Technical Library CI 290/36-84 AUTO-Sutton	1
Professor G. Whitesides Department of Chemistry Massachusetts Institute of Technology Cambridge, Massachusetts 02139	1	Dr. E. Baer Department of Macromolecular Science Case Western Reserve University Cleveland, Ohio 44106	1
Professor J. Wang Department of Chemistry University of Utah Salt Lake City, Utah 84112	1	Dr. K. D. Pae Department of Mechanics and Materials Science Rutgers University New Brunswick, New Jersey 08903	1
Dr. V. Stannett Department of Chemical Engineering North Carolina State University Raleigh, North Carolina 27607	1	NASA-Lewis Research Center 21000 Brookpark Road Cleveland, Ohio 44135 Attn: Dr. T. T. Serofini, MS-49-1	1
Dr. D. R. Uhlmann Department of Metallurgy and Material Science Massachusetts Institute of Technology Cambridge, Massachusetts 02139	1	Dr. Charles H. Sherman, Code TD 121 Naval Underwater Systems Center New London, Connecticut	1
Naval Surface Weapons Center White Oak Silver Spring, Maryland 20910 Attn: Dr. J. M. Augl Dr. B. Hartman	1	Dr. William Risen Department of Chemistry Brown University Providence, Rhode Island 02192	1
Dr. G. Goodman Globe Union Incorporated 5757 North Green Bay Avenue Milwaukee, Wisconsin 53201	1	Dr. Alan Gent Department of Physics University of Akron Akron, Ohio 44304	1

TECHNICAL REPORT DISTRIBUTION LIST, 356A

	<u>No. Copies</u>		<u>No. Copies</u>
Mr. Robert W. Jones Advanced Projects Manager Hughes Aircraft Company Mail Station D 132 Culver City, California 90230	1	Dr. T. J. Reinhart, Jr., Chief Composite and Fibrous Materials Branch Nonmetallic Materials Division Department of the Air Force Air Force Materials Laboratory (AFSC) Wright-Patterson Air Force Base, Ohio	1 4543
Dr. C. Giori IIT Research Institute 10 West 35 Street Chicago, Illinois 60616	1	Dr. J. Lando Department of Macromolecular Science Case Western Reserve University Cleveland, Ohio 44106	1
Dr. M. Litt Department of Macromolecular Science Case Western Reserve University Cleveland, Ohio 44106	1	Dr. J. White Chemical and Metallurgical Engineering University of Tennessee Knoxville, Tennessee 37916	1
Dr. R. Y. Roe Department of Materials Science and Metallurgical Engineering University of Cincinnati Cincinnati, Ohio 45221	1	Dr. J. A. Manson Materials Research Center Lehigh University Bethlehem, Pennsylvania 18015	1
Dr. Robert E. Cohen Chemical Engineering Department Massachusetts Institute of Technology Cambridge, Massachusetts 02139	1	Dr. R. F. Helmreich Contract RD&E Dow Chemical Co. Midland, Michigan 48640	1
Dr. David Roylance Department of Materials Science and Engineering Massachusetts Institute of Technology Cambridge, Massachusetts 02039	1	Dr. R. S. Porter University of Massachusetts Department of Polymer Science and Engineering Amherst, Massachusetts 01002	1
Dr. T. P. Conlon, Jr., Code 3622 Sandia Laboratories Sandia Corporation Albuquerque, New Mexico	1	Professor Garth Wilkes Department of Chemical Engineering Virginia Polytechnic Institute and State University Blacksburg, Virginia 24061	1
Dr. Martin Kaufmann, Head Materials Research Branch, Code 4542 Naval Weapons Center China Lake, California 93555	1	Dr. Kurt Baum Fluorochem Inc. 6233 North Irwindale Avenue Azusa, California 91702	1
Professor S. Senturia Department of Electrical Engineering Massachusetts Institute of Technology Cambridge, Massachusetts 02139	1	Professor C. S. Paik Sung Department of Materials Sciences and Engineering Room 8-109 Massachusetts Institute of Technology Cambridge, Massachusetts 02139	1